



**HAL**  
open science

## Self-coacervation of ampholyte polymer chains as an efficient encapsulation strategy.

Adeline Perro, Lauriane Giraud, Noémie Coudon, Sharvina Shanmugathasan, Véronique Lapeyre, Bertrand Goudeau, Jean-Paul Douliez, Valérie Ravaine

► **To cite this version:**

Adeline Perro, Lauriane Giraud, Noémie Coudon, Sharvina Shanmugathasan, Véronique Lapeyre, et al.. Self-coacervation of ampholyte polymer chains as an efficient encapsulation strategy.. Journal of Colloid and Interface Science, 2019, 548, pp.275-283. 10.1016/j.jcis.2019.04.033 . hal-02628923

**HAL Id: hal-02628923**

**<https://hal.inrae.fr/hal-02628923>**

Submitted on 26 Oct 2021

**HAL** is a multi-disciplinary open access archive for the deposit and dissemination of scientific research documents, whether they are published or not. The documents may come from teaching and research institutions in France or abroad, or from public or private research centers.

L'archive ouverte pluridisciplinaire **HAL**, est destinée au dépôt et à la diffusion de documents scientifiques de niveau recherche, publiés ou non, émanant des établissements d'enseignement et de recherche français ou étrangers, des laboratoires publics ou privés.



Distributed under a Creative Commons Attribution - NonCommercial 4.0 International License

# Self-coacervation of ampholyte polymer chains as an efficient encapsulation strategy

Adeline Perro<sup>1,\*</sup>, Lauriane Giraud<sup>1</sup>, Noémie Coudon<sup>1</sup>, Sharvina Shanmugathan<sup>1</sup>, Véronique Lapeyre<sup>1</sup>, Bertrand Goudeau<sup>1</sup>, Jean-Paul Douliez<sup>2</sup> and Valérie Ravaine<sup>1</sup>

<sup>1</sup> Université de Bordeaux, Bordeaux INP, ISM, UMR 5255, Site ENSCBP, 16 avenue Pey Berland, 33607 Pessac, France.

<sup>2</sup> UMR1332, Biologie du Fruit et Pathologie, INRA, univ. Bordeaux, Centre de Bordeaux, 33883, Villenave d'Ornon, France.

\*Corresponding author: [adeline.perro@enscbp.fr](mailto:adeline.perro@enscbp.fr)

## Abstract

Coacervation is a phase separation process involving two aqueous phases, one solute-phase and one solute-poor phase. It is frequently observed among oppositely-charged polyelectrolyte systems. In this study, we focus on self-coacervation involving a single polymer chain and investigate its potential for encapsulation applications.

Negatively charged polyacrylic acid polymer chains were partially cationized using diamine and carbodiimide chemistry affording ampholytes, named PAA-DA, with tunable charge ratio. When dispersed in water, at pH 7, PAA-DA was soluble but a phase separation occurs when decreasing pH close to the isoelectric point. Coacervation is found only for a given amine-to-acid ratio otherwise precipitation is observed. Increasing the pH above 4 yielded progressive destruction of the coacervates droplets via the formation of vacuoles within droplets and subsequent full homogeneous redispersion of PAA-DA in water. However, addition of calcium allowed increasing the coacervate droplet stability upon increasing the pH to 7 as the divalent ion induced gelation within droplets.

Moreover, the coacervate droplets present the ability to spontaneously sequester a broad panel of entities, from small molecules to macromolecules or colloids, with different charges, size and hydrophobicity. Thanks to the reversible character of the coacervates, triggered-release could be easily achieved, either by varying the pH or by removing calcium ions in the case of calcium-stabilized coacervates. Self-coacervation presents the advantage of pathway-independent preparation, offering a real output interest in pharmacy, water treatment, food science or diagnostics.

### **Keywords**

Water-in-water emulsion, Sequestration, Self-coacervation

## 1. Introduction

Coacervation refers to a phase separation directed by electrostatic interactions of charged molecules in aqueous environment. Coacervates form turbid solutions made of micrometric liquid droplets having a spherical shape that generally coalesce, further yielding macroscopic phase separation. Two types of coacervation phenomenon are distinguished: the complex coacervation and the simple or self coacervation.

Complex coacervation results from the complexation between two electrolytes of opposite charge and is commonly described in the literature.[1] Binary mixtures of biological (DNA, proteins fatty acid, polysaccharides ...) and synthetic compounds (polymers, surfactants, polyelectrolytes) can form complex coacervates.[2-8] Despite the multiple pathways available to understand coacervation processes in these systems, the control of such phase separation is still challenging.[9-11]

Self-coacervation is a phase separation resulting from the loss in solvency of a single macromolecule, where the driving force is related to the charge balance that occurs varying the pH, ionic strength or temperature.[12,13] In contrast to complex coacervation, few examples, mostly exploiting proteins are found in the literature.[14,15] For instance, adhesive systems used in many marine organisms such as mussels constitute a natural example of self-coacervation, where the loss of solvency is directed by a strong cation- $\pi$  interaction in saline water.[16-18]

In both cases of complex and self-coacervation, the polymers are concentrated within the liquid droplets embedded in a continuous water phase that may contain diluted polymers in equilibrium. The phenomenon strongly depends on the charge ratio, the ionic strength and the pH that trigger the interactions between polymer chains or intra-chain interactions.

Mixtures of opposite charged polymers may also lead to aggregation or precipitation phenomenon that is different to the coacervation phenomenon. In a such a case, a solid is formed and droplets are no longer observed. These amorphous solid particles constitute a limitation in terms of applications as their physico-chemical properties are completely different from coacervates. A milestone is to study in details the polymer interactions as these two phenomenon results from a fragile equilibrium.[19,20]

Coacervates are of fundamental interest for understanding their formation and offer practical applications since they are able to sequester chemicals. Indeed, they have the ability to spontaneously sequester components of interest ranging from small molecules to living

cells.[21,22] Moreover, such approaches in all-aqueous media, offer a mild environment for many applications as the design of bioreactors, protocells or organelles.[23-25]

In this work, we have exploited a synthetic polymer chain that bears both positively and negatively charges by grafting amine groups on a polyacrylic acid polymer chain *via* carbodiimide-chemistry. The ratio of the polymer charges was controlled by the grafting degree of the ampholyte and the pH of the solution. The self-coacervation is generated close to the isoelectric point of the ampholyte polymer with no additional molecules. This investigation highlighted the existence of an equilibrium between the coacervation and precipitation phenomena occurring generally in complex coacervation.

Additionally, these micrometric coacervates have the ability to spontaneously sequester various entities presenting different charges or hydrophobicity degrees. The spontaneous and reversible sequestration in such coacervates was investigated by fluorescence spectroscopy. We have also observed the formation of vacuoles, which are characteristic of a metastable state by slowly modifying the pH of the solution. Finally, we have increased the stability of the coacervates at neutral pH, upon addition of calcium ions, which induced gelation of the polymer within droplets.

## 2. Materials and methods

### 2.1. Materials

N,N'-dimethylethylenediamine (98%), 1-Ethyl-3-(3-dimethylaminopropyl) carbodiimide hydrochloride (EDC, >98%), calcium chloride (CaCl<sub>2</sub>), Ethylenediaminetetraacetic acid (EDTA), fluorescent dyes such as rhodamine B, Fluorescein isothiocyanate (FITC), coumarin, Diethylaminoethyl (DEAE)-Dextran (3-4kDa and 150kDa), Carboxymethyl (CM)-Dextran (150kDa), Dextran-Rhodamine B (10 and 70kDa) were purchased from Sigma-Aldrich. Polyacrylic acid (25 wt% solids in water Mn= 50,000 g/mol) was purchased from Polysciences.

### 2.2. Methods

#### 2.2.1. PAA-DA<sub>x</sub> polymer chains

##### 2.2.1.1. Synthesis of ampholyte polymer chains

At room temperature, 3.0 mmol of PAA 25w% solids in water (Mn=50 kDa) were dissolved in 15 mL of milliQ water. 9 mL of solution of N,N'-dimethylethylenediamine (from 0.05 to 0.40 eq/Carboxylic groups) were introduced in the mixture. The pH was adjusted to 6 using NaOH (1 M). A solution of EDC (1.1 mmol, 0.4 eq/Carboxylic groups, 6 mL) was prepared independently and the pH was fixed to 5-6. The EDC solution was then added dropwise in the PAA/N,N'-dimethylethylenediamine mixture. The solution was stirred for at least 1h.

A purification procedure of the ampholyte polymer chains was done by a precipitation process in a mixture of acetone and water (2/1 vol.) in presence of salt (NaCl = 100 mM). The precipitate was recovered and further dissolved and dialyzed against water. The purified polymer was recovered by freeze-drying.

##### 2.2.1.2. Proton nuclear magnetic resonance

<sup>1</sup>H NMR spectra in D<sub>2</sub>O (C = 10 mg.mL<sup>-1</sup>) were recorded at 300 K with 16 scans using a Bruker 400 MHz spectrometer. The degree of functionalization was determined by the integration of the grafted diamine signal relative to the signal of polyacrylic acid (Table S1). Various polymers were synthesized, named PAA-DA<sub>x</sub>, where x represents the degree of

diamine functionalization ranging from 5 to 40% relative to the number of carboxylic acid groups.

#### 2.2.1.3. Potentiometric titrations of PAA-DA<sub>x</sub> polymer chains

Potentiometric titrations were done in order to investigate the pH dependence of the PAA-DA<sub>x</sub> polymer chains. The positive to negative ratio was determined *via* the analysis of the degrees of ionization of carboxylic and diamine groups. PAA-DA<sub>x</sub> solutions were prepared at a concentration of 5 g.L<sup>-1</sup> (pH = 6.15). Titrations of 15 mL of the PAA-DA<sub>x</sub> solution were performed with 0.1 M HCl at room temperature.

### 2.2.2. Self-coacervation of ampholyte polymer chains

#### 2.2.2.1. Fabrication of PAA-Dax coacervates

0.5%wt of PAA-DA<sub>x</sub> polymer chains were dissolved in a MES buffer (pH=6) at 4°C. The pH of the solution was decreased until the apparition of turbidity, related to the coacervation process. The solution was kept at 4°C before characterization.

#### 2.2.2.2. Microscopic observation

Bright field images were obtained using a Zeiss microscope (Image M1). Confocal microscopy imaging was performed using a Leica TCS-SP5 inverted microscope equipped with a laser source and a spectral selector module in front of the photomultiplier tube (PMT) detector. SEM images were acquired on a Hitachi TM-1000 field emission scanning electron microscope with a 15.0 kV voltage. The samples were prepared as follow: a drop containing coacervates was deposited on a glass slide and freeze-dried to preserve the fragile structure.

#### 2.2.2.3. Turbidimetric titrations

The turbidimetric titrations were carried out at 600 nm by using a UV spectrometer (Varian – Cary 100 scan UV-Visible spectrophotometer). The pH and the transmittance were monitored 30 minutes after the mixing procedure.

#### 2.2.2.4. Surface charges measurements

The Zeta potential of the colloids was measured using Zetasizer Nanoseries (Malvern) *via* 4 mW He/Ne laser (632.8 nm wavelength) with a scattering angle of 175° and the temperature was set at 25 °C. Samples were prepared by dispersing 0.5 %wt of a solution containing coacervates at pH=3.5.

#### 2.2.3. Sequestration of chemical entities in coacervates

Entities of interest (molecules, macromolecules or latex [26]) were introduced in a stock solution of PAA-DA<sub>x</sub> (0.5 %wt, pH=6, no coacervates). Then, the pH of the solution was decreased to 3.5 to form coacervates. Direct observations were performed using bright field and fluorescence microscopies.

In order to quantify the molecular sequestration, two solutions containing 12.5µg/L of fluorescently labeled molecules in MES buffer were fabricated. As the first one constitutes the reference, the other contained PAA-DA<sub>x</sub> ampholyte chains (0.5 wt%). The pH of both solutions was decreased to 3.5 before centrifugation at 500 rpm during 15 minutes. 100µL of the supernatant were dispersed in 2mL of a buffer solution at pH 7 prior to spectroscopic fluorescence characterization.

#### 2.2.4. Stabilization of the coacervates at neutral pH

The stabilization of the coacervates at neutral pH was carried out by introducing a chemical linker. 75 µL of a solution of CaCl<sub>2</sub> (1 M) was introduced in 2mL of a solution containing coacervates at pH 3.5. The solution was rested at least 3 hours before the slow increase of the pH towards the pH of the MES buffer (~6).



### 3. Results and discussion

#### 3.1. Preparation of PAA-DA<sub>x</sub> ampholyte polymer chains

A poly-acrylic acid (PAA) polymer chain was modified by grafting a diamine group through an 1-Ethyl-3-(3-dimethylaminopropyl)carbodiimide) –EDC- coupling (Figure 1A). The diamine randomly reacted only at one end on some carboxylate groups of PAA to yield an amide bond, whereas the other end provided a free amine group. The amine group was positively charged at a pH below its pK<sub>a</sub>, *i.e.* 10.5, whereas the carboxylic group of PAA was negatively charged at a pH above 4.2 (pK<sub>a</sub> for poly(acrylic acid), from chemical Handbook). Controlling the initial amount of the diamine groups compared to the carboxyl groups led to the fabrication of several ampholyte polymers with different ratio of positive and negative charges. After purification steps to remove excess diamine, ampholyte PAA-DA<sub>x</sub>, with *x* ranging from 5 to 40 were obtained.

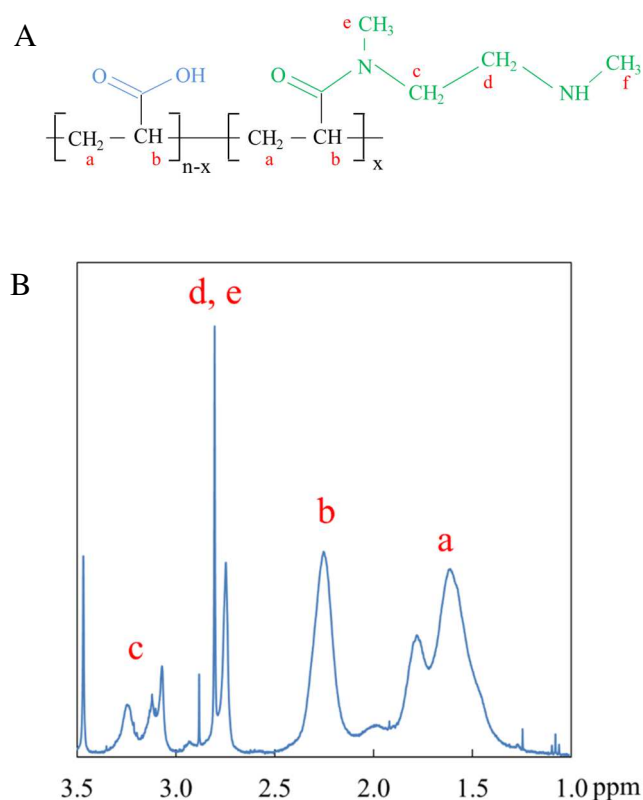


Figure 1: A) Chemical structure of PAA-DA<sub>x</sub> ampholyte polymer. B) <sup>1</sup>H-NMR spectrum of PAA-DA<sub>10</sub> (ppm): 1.3-2.0 (4H, -CH<sub>2</sub>, PAA), 2.1-2.3 (2H, -CH, PAA), 2.7 (3H, -CH<sub>3</sub>, DA), 2.9 (3H, -CH<sub>3</sub>, DA), 3-3.3 (4H, -CH<sub>2</sub>, DA). a, b, c, d, e, f represent equivalent protons as indicated on the chemical structure (A).

The resulting diamine-grafted PAA (PAA-DA<sub>x</sub>) was characterized by <sup>1</sup>H-NMR and as an example, we present the spectrum for x=10 (Figure 1B). The chemical shifts at 1.3–2.5 ppm were attributed to the protons of the PAA polymer chain (a and b) whereas the others (c, d, e and f) were assigned to the diamine moiety (see also Figure S1).

Once the spectra obtained, digital integrations for each peak were performed, allowing measuring the degree of functionalization (Table S1). The resulting experimental values are in accordance with the number of chemical groups initially introduced in the solution.

### **3.2. Phase separation of PAA-DA<sub>x</sub>, precipitation versus coacervation**

We have selected ampholyte polymer chains with various degree of functionality from 5 to 40%. Each ampholyte polymer chain was dispersed in deionized water at a pH of 6 ([PAA-DA<sub>x</sub>] = 5g/L). Decreasing pH lead to two different behaviors: i) For PAA-DA<sub>x</sub> with x ranging from 10 to 25, a cloudy solution, corresponding to a phase separation in the aqueous solution, appeared in a range of pH from 3.0 to 4.5. This phenomenon was highlighted by the open marks on the phase diagram in Figure 2. ii) For x below 5 and above 30, the phase separation never occurred as the solution remained limpid whatever the pH.

It appears that the ratio between positively and negatively charged groups plays a fundamental role on the occurrence of the phase separation by varying the pH. These results can be compared to the phenomenology occurring in mixtures of two oppositely-charged polymers. Indeed, beyond the appropriate charge ratio range, the polymer chains do not interact, leading to a solubilization of the polymer rather than their assembly.<sup>27</sup>

Exploiting the potentiometric titration, we determined the value of the isoelectric point (IEP) of the ampholyte chain. We found 3.2 for a modification of 15%, 3.5 for 20% and 3.7 for 25%. Grafting a higher amount of amine groups yielded a shift of the IEP towards higher values, consequently increasing the positive to negative charge ratio.

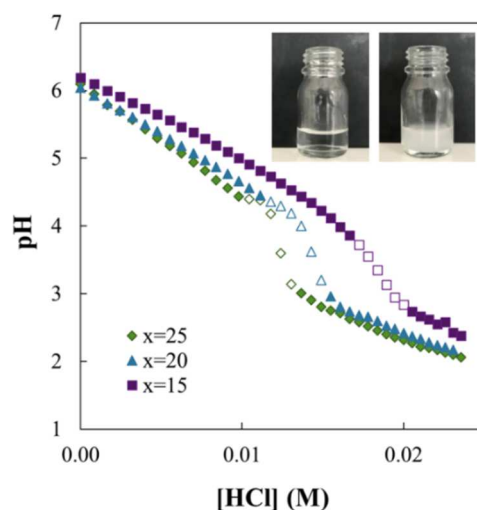


Figure 2: Potentiometric titration of the PAA-DA<sub>x</sub> (0.25 mM). Diamond, x= 25; triangle, x= 20; Square, x= 15. [PAA-DA<sub>x</sub>]= 5 g/L, Titrant solution: [HCl]=0.1M. The phase separation is highlighted by open marks. Inset: Photos of sample vials out of the phase separation regime (left, limpid) and in the two-phases domain (right, turbid).

We then more deeply studied the turbid samples obtained at the pH of the IEP to determine whether coacervation or precipitation phenomenon occurred in these experimental conditions.[28] The samples were directly visualized by microscopy and freeze-dried before their observation by SEM. For PAA-DA<sub>15</sub>, spherical droplets with micrometric dimensions were observed as shown in Figure 3 A&B. These polymer-rich droplets were identified to be coacervates, regarding their smooth, spherical and regular surface. Their diameter distribution, centered at 3.5 μm, was quite large, with a standard deviation of 1.4 μm as shown in Figure S2. In order to confirm that these drops contained concentrated polymers, PAA-DA<sub>15</sub> were fluorescently labelled with fluoresceinamine *via* EDC coupling chemistry. 0.02%wt of this fluorescent ampholyte were mixed with non-labelled polymer chains and dispersed in the buffer (PAA-DA<sub>15</sub> = 0.5%wt), after what, the pH was decreased to 3.5 to form coacervates. Confocal fluorescence microscopy showed fluorescent droplets embedded in a continuous phase lacking fluorescence showing that the ampholyte chains were indeed concentrated within the droplets (Figure 3C&D). Coacervation is a process resulting in macroscopic phase separation. To probe the equilibrium nature of the coacervate phase, the drops were centrifuged at 500 rpm for 10 min and the sediment was observed by microscopy. Dispersed droplets were found to coexist with large domains of polymer rich phase,

which tended to stick onto the glass slide (Figure S3A), showing the occurrence of macroscopic phase separation. Finally, the reversibility of the process was demonstrated by varying the pH following different pathway around the isoelectric point. Figure S3B demonstrates the accordance of the pH variation in direct or reverse potentiometric titration.

PAA-DA<sub>25</sub> led to a different kind of objects, which are not easily discernable with conventional microscopy (Figure 3E). SEM pictures presented Figure 3F revealed the presence of submicronic objects presenting an angular shape, which were identified to be precipitates. As the transition from coacervates to precipitates depends on the strength of attractive interactions, [29] the charge ratio of positive to negative groups directs the local interactions of the polymer chains.

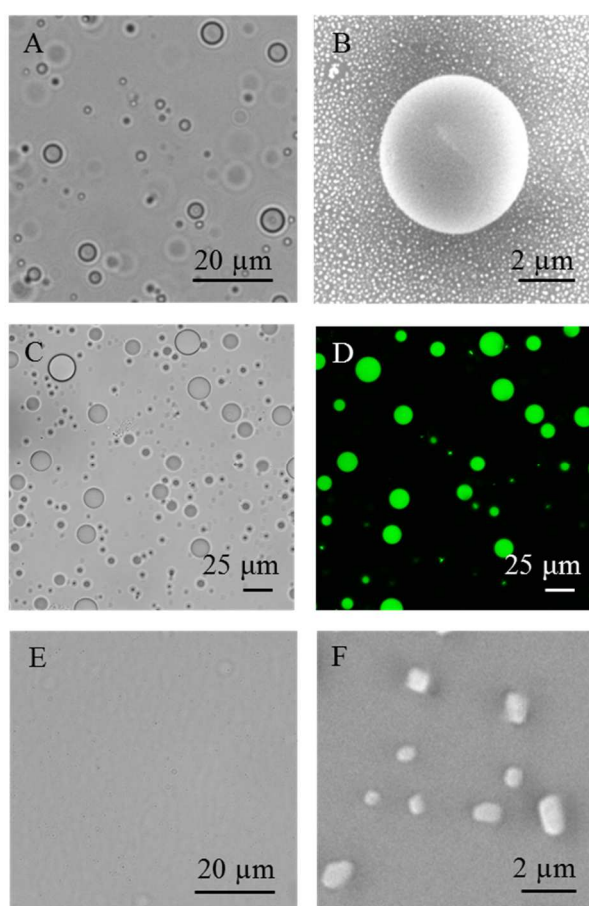


Figure 3: Images of coacervates (PAA-DA<sub>15</sub>, pH=3.5). A) Optical microscopy B) SEM view after freeze drying. Images of coacervates using FITC- labeled PAA-DA<sub>15</sub>, (pH=3.5) C) Optical microscopy, D) Confocal microscopy. Images of precipitates E) Optical microscopy, F) SEM view after freeze drying of precipitates (PAA-DA<sub>25</sub>, pH=3.7).

We then studied whether both precipitation and coacervation phenomenon can occur for a given value of  $x$ . For this, we analyzed the variation of turbidity ( $\tau$ ) and the charge surface as a function of pH. These results are presented in Figure 4 A for PAA-DA<sub>15</sub> solution (0.5%wt) and in Figure S4, the IEP was at pH 3.2. As the coacervation phenomenon is directed by the positive to negative charge ratio, we achieved the quantification of negative charges assuming that all the diamine functions were in the ionized state at a pH below 5, *i.e.*  $[\text{NH}_3]_{\text{Introduced}}=[+]$ . The degree of ionization of the carboxylic groups  $\alpha$  at various pH was determined by exploiting the modified Henderson-Hasselbalch equation [30] and the results are presented in Figure 4:

$$pK_a = pH + \log \frac{(1-\alpha)}{\alpha} \quad (1)$$

$$\alpha = \frac{[\text{COO}^-]}{[\text{COOH}]+[\text{COO}^-]} \quad (2)$$

The pH of the solution, initially at 6.15, was slowly decreased toward the apparition of a turbid solution, which occurred at pH 4.2. Microscopic observations (Figure S5 A) showed that precipitates are mainly formed. Then, decreasing the pH to 3.2 induced an increase of the number of observed coacervates over the precipitates (Figure S5 B). This transition is noticeable with a decrease of the turbidity at a pH closed to the isoelectric point of the polymer chain (pH=3.2 for PAA-DA<sub>15</sub>). Finally, the dissolution of the coacervates was observed at pH 2.5 since the solution became limpid again.

Typically, the complex coacervation occurs close to the isoelectric point of the polymer, when the complexes exhibit zero net charge. As mentioned previously, the self-coacervation of PAA-DA<sub>x</sub> occurs at a pH closed to the IEP of the polymer chain. Investigating the zeta potential of PAA-DA<sub>15</sub> coacervates showed that at the pH of coacervation, the charge surface is far from zero ( $\xi=-13$  mV), traducing that the coacervates are formed with a slight excess of negative charges. This original result could be explained following Frederickson *et al.* work in which self coacervation of block polyampholyte was investigated. These polymer chains formed isolated charged globules leading to a neutral coacervate as illustrated in Figure 4B (top).[10,31,32] In the case of our ampholyte polymer chain, we can suggest a random distribution of the positive charges onto the polymer chain. At the pH of coacervation, the

diamine groups create electrostatic bridges with the charged carboxylic groups.[33] These intra-chain interactions yield the formation of a global negatively charged complex as schematically represented Figure 4B (Bottom). Moreover, the random dispersion of the positive charges along the PAA chain favor the formation of polymer loops, which maintain a certain level of hydration. This phenomenon was also observed with complex coacervation of weak flexible polymer chains, which limit the formation of charged globules leading to a charge ratio, *i.e.*  $[\text{COO}^-]/[\text{NH}_3^+]$  far from the stoichiometry.[27]

From these observations, we can establish that self-coacervation is observed in presence of a small excess of negative charges, which can be control by the pH *via* the protonation of the carboxylic negative charges.

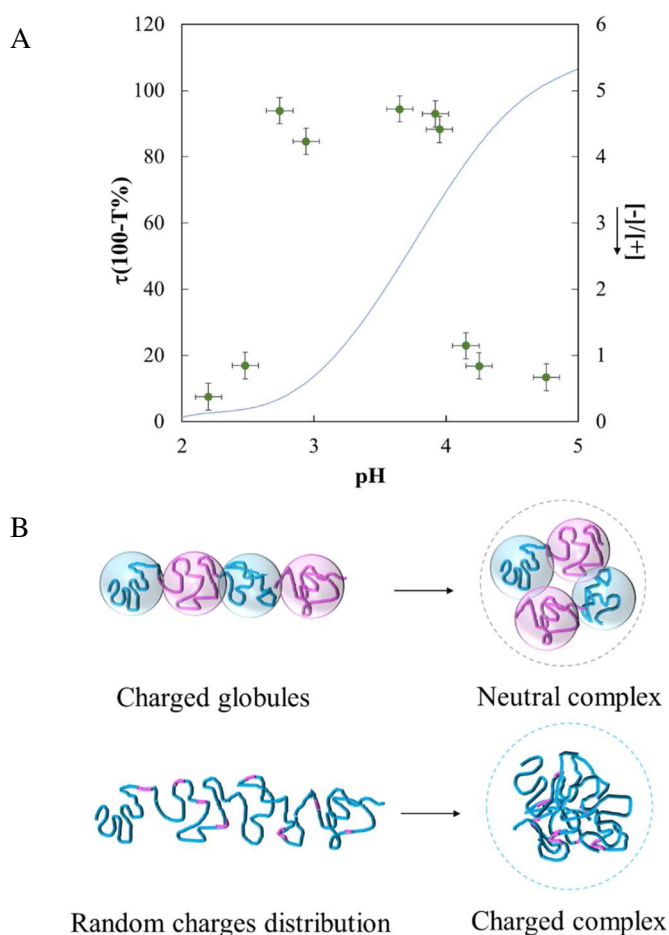


Figure 4: A) Turbidity measurements (green marks) and charge ratio of positive to negative groups (blue curve) for PAA-DA<sub>15</sub> (0.5wt%) as a function of pH. B) Schematic representation of the formation of coacervates. Negative charges are represented in blue and positive charges in pink.

We have schematically presented in Figure 5, the transitions occurring in the self-coacervation process presented in this work. This phase diagram shows that biphasic domains were obtained by monitoring the grafting density of the polymer chain and the pH of the solution (gray domain). Moreover, we have highlighted the domains where the coacervation was predominant over precipitation. In the light of these observations, self-coacervation results from a delicate equilibrium between precipitation, coacervation and polymer dispersion state.

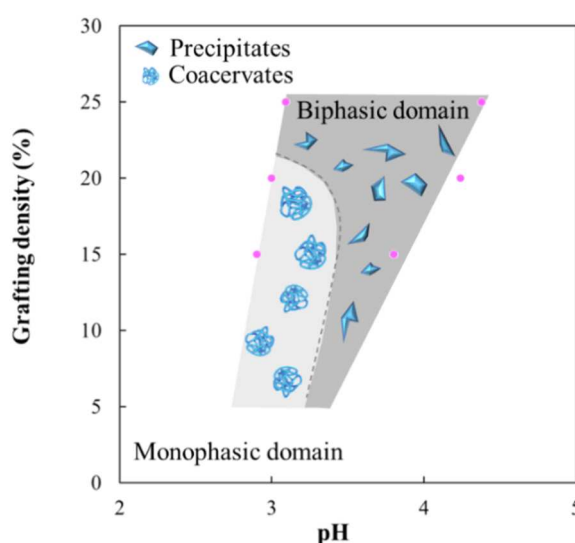


Figure 5: Phase diagram of the different phase regions observed by varying the grafting density and the pH of the solution. The pink points correspond to the pH of the apparition of a cloudy solution extracted from Figure 2.

### 3.3. Stability of PAA-DAX coacervates

We first investigated the stability of the coacervates over time. Interestingly, their size remained stable during more than 12 days when stored at 4°C at pH 3.2 (Figure S6). As mentioned previously, increasing the pH above 4.2 induced the destruction of the coacervates. We analyzed this destruction phenomenon in details by slowly increasing the pH of a solution containing FITC labeled PAA-DA<sub>20</sub> coacervates. Experimentally, we created a pH gradient by depositing a droplet of a basic solution (NaOH=0.1 M) in contact with a droplet of coacervates and observed the coacervation destruction under a

microscope. Fluorescent microscopy revealed the occurrence of fluctuations in size and shape exhibiting non-fluorescent domains containing water molecules extracted from the continuous media also called vacuoles (Figure 6).

We observed a random nucleation of these vacuoles at the surface of the droplet, which merged before the complete destruction of the coacervate (SI movie). This phenomenon of vacuolization was already observed for complex coacervates placed under an electric field.[34,35] In both cases, the vacuolization is driven by an asymmetric osmotic pressure resulting from a local modification of ions concentration. Moreover, the stabilization of the vacuolated coacervates could open a route for the development of compartmentalized structures.[36-39]

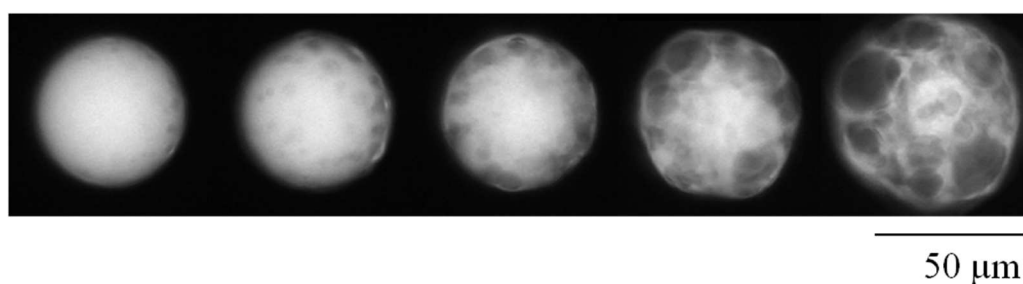


Figure 6: Optical microscopic images obtained by increasing the pH. PAA-DA<sub>20</sub> were labeled with FITC. A droplet of NaOH (0.1M) was deposited closed to the coacervate under the microscope objective.

In order to increase the robustness of the coacervates at neutral pH, an additional cross-linker is needed. This was achieved by introducing Ca<sup>2+</sup> cations, which are well-known to form ionic bridges between ionized carboxylic group. In a typical experiment, 0.04 M of CaCl<sub>2</sub> was introduced in a solution containing coacervates at pH 3.2 as illustrated Figure 7A. Once calcium was added the persistence of the polymer-enriched droplets was observed after raising pH to 7.[40] These gelled droplets were then centrifuged and dispersed in deionized water. Interestingly, they kept their integrity, and remained stable for several weeks (Figure S7). Their zeta potential was measured. It was only slightly negative ( $\xi=-0.4$  mV). Thus, it was much higher than that before calcium addition at pH 3, despite the deprotonation of carboxylic functions upon pH increase. This suggests that Ca<sup>2+</sup> were effectively incorporated in the structure.

Finally, we investigated the destruction of the Ca<sup>2+</sup>-stabilized coacervates. EDTA is a common sequestering agent for Ca<sup>2+</sup>. Therefore, the stability of the Ca<sup>2+</sup>-stabilized



coacervates was probed in the presence of EDTA. Figure 7B shows the flow of an EDTA solution (0.2 M) diffusing in a solution of  $\text{Ca}^{2+}$ -stabilized coacervates at neutral pH. It worth noticing that in presence of EDTA, the coacervates presents vacuoles during the destruction process as observed previously with non-gelled coacervates upon increasing the pH.

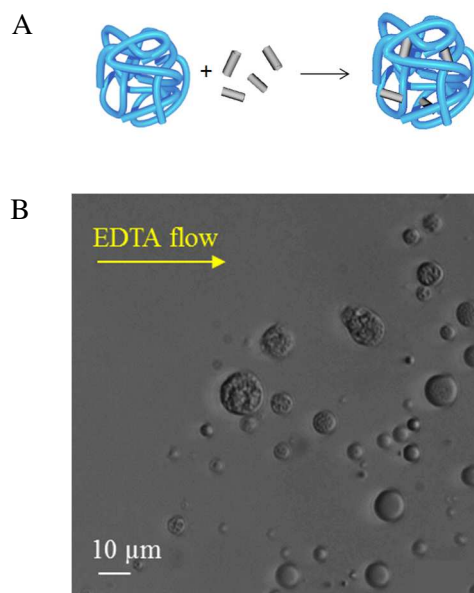


Figure 7: A) schematic representation of coacervate stabilization using ionic bridges; B) Optical microscopy image of the destruction of PAA-DA<sub>x</sub> @  $\text{Ca}^{2+}$  in presence of EDTA (0.2 M).

### 3.4. Sequestration in PAA-DA<sub>x</sub> coacervates

Finally, the ability of PAA-DA<sub>15</sub> to sequestrate various compounds was investigated. A range of compounds including small molecules, macromolecules or colloids was probed. In a typical experiment, a known amount (1 mg) of a fluorescently labeled chemical entity was introduced in 5 mL of a stock solution at pH=5. The pH was decreased to 3.5 to form the coacervates before its observation by optical and fluorescence microscopy, which are presented in Table S2 and in Figure 8. In a first set of experiments, rhodamine (positively charged, +), FITC (negatively charged, -) or coumarin (uncharged, 0), which are small molecules (<500 Da) were introduced.

Although these molecules present different charges at neutral pH, the sequestration is observed for each molecule, even if, visual differences could be distinguished in the

partition coefficient. Similar experiments were done using macromolecules such as FITC-DEAE-Dextran (3-4 kDa and 150 kDa) and FITC -CM-Dextran (150 kDa), which are positively and negatively charged, respectively. As observed above, coacervates are loaded with dextran molecules whatever their charge (Table S2 and Figure 8). Finally, the process was extended to colloidal particles such as negatively charged latex beads ( $D = 115$  nm). It is clearly observed in Figure 8 that the polystyrene latex were localized inside the coacervates. These results demonstrate that the molecular charge and the size are not the prevalent parameters in the sequestration efficiency.[41]

We investigated in more details the role of the molar mass of macromolecules onto the sequestration efficiency. To do so, we have studied by fluorescence spectroscopy the partition coefficient of a small molecule such as the Rhodamine B (<500 Da) and two macromolecules, which are Dextran Rhodamine 10 kDa and 70 kDa.

Two solutions containing the fluorescently labeled molecules in presence and in absence of PAA-DA<sub>15</sub> were prepared. Then, the pH of the solutions was adjusted at the pH of coacervation. After centrifugation, we measured the fluorescence of the supernatant of the two solutions. The ratio of the two measured fluorescence intensities was then calculated. As more than 60% of small molecules were loaded, the sequestration efficiency decreased to ~30% for dextran 10 kDa and reach only ~20% for dextran 70 kDa. The detailed results are presented in Table S3.

From these observations, the parameters that direct the sequestration efficiency are not completely understood as the partition coefficient is not mainly directed by the charges, dimensions or hydrophilicity of the molecules. Nevertheless, none of parameters studied herein have presented the total exclusion of the molecules from the coacervates.

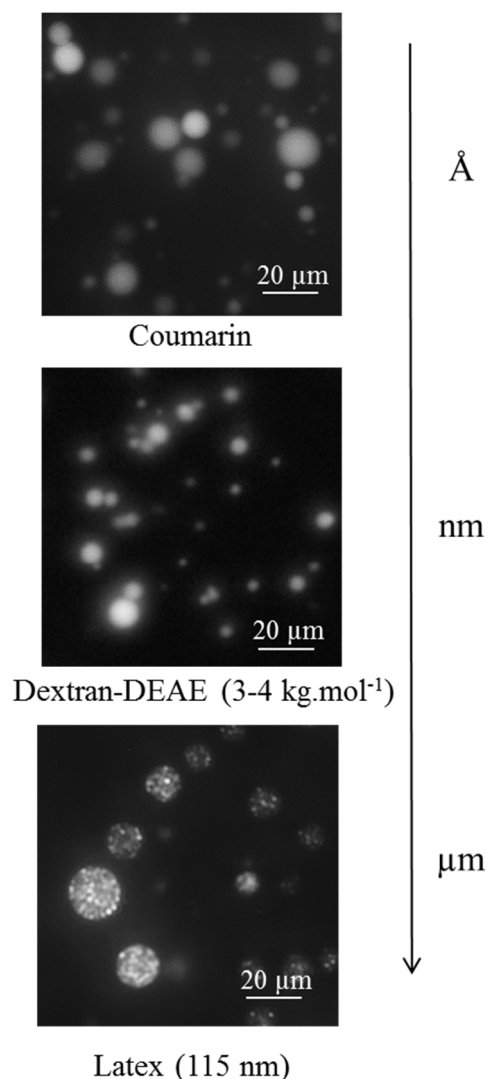


Figure 8: Fluorescent images of coacervates with small molecules (coumarin), macromolecules (Dextran, 3-4 kg/mol, DEAE), colloids (latex beads).

We investigated the reversible character of the sequestration phenomenon. At a pH out of the domain of coacervate formation, the solution was clear, *i.e.* the ampholyte polymer chain and a fluorescent dye (rhodamine B) were soluble in the solution. A known volume of the solution was taken and dispersed in a buffer solution (pH = 7). The fluorescence intensity of the resulting solution was measured by fluorescent spectroscopy, giving the initial measured fluorescence intensity.

Then, the pH was decreased to form coacervates, yielding sequestration of the fluorescent dye as already commented above and presented in Figure 9A. The solution was centrifuged and the fluorescence of the supernatant was measured as presented

before. Several cycles of destruction/formation of coacervates for a given sample were realized and are presented Figure 9B. It shows that the fluorescence intensity decreases radically in presence of coacervates up to 60% for the first cycle. Increasing the pH allow the regeneration of the initial fluorescence intensity. A decrease to 40% was observed for the three following cycles, showing the reversible character of the sequestration process. Several cycles of pH variation were performed allowing the destruction and the reformation of the coacervates. Obviously, at each cycle, the factor of dilution of the PAA-DA<sub>10</sub> and the ionic strength of the solution increased because of the consecutive addition of NaOH and HCl.

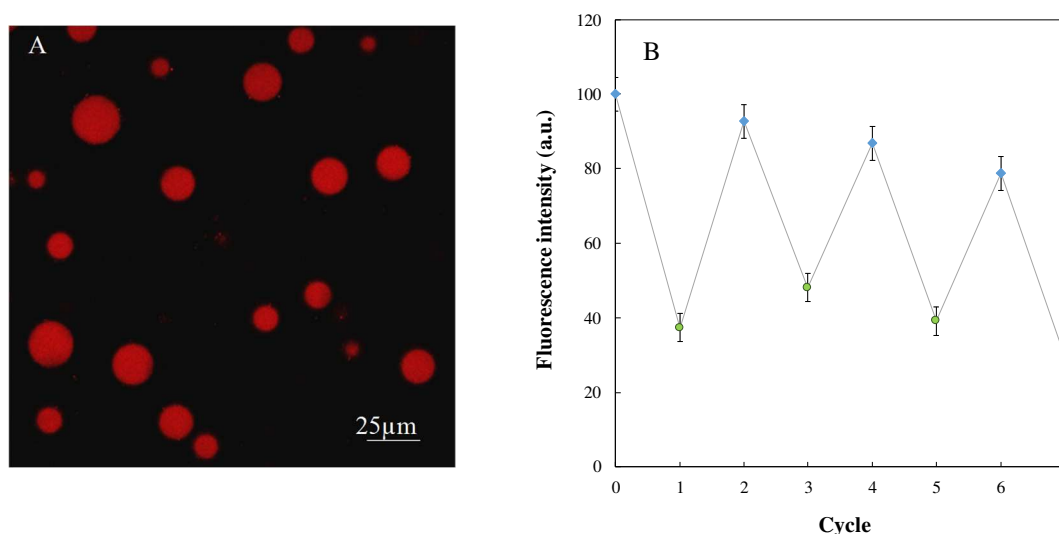


Figure 9: A) Confocal image of coacervates PAA-DA<sub>10</sub> containing rhodamine. B) Fluorescence intensity variation of the supernatant in presence (green circles) and in absence of coacervates (blue diamond), pH = 7,  $m_{\text{PAA-DA10}} = 5 \text{ mg.mL}^{-1}$ .

Moreover, we observed that the sequestration efficiency was identical whatever the experimental pathway, *i.e.* incorporation of the dyes before or after the coacervates formation. The remarkable sequestration ability of the coacervates gives them as interesting candidates for the fabrication of versatile cargos.[42]

Finally, we investigated the sequestration ability of PAA-DA<sub>15</sub> coacervates stabilized by Ca<sup>2+</sup>. Fluorescent dyes (coumarin and fluorescently labelled polystyrene beads) were introduced in the solution containing the polymer chains at neutral pH. After the coacervates formation, calcium was further added yielding to their gelation. Then, pH was slowly increased. At pH 7, the polystyrene beads, initially sequestered in the coacervates, remained in the polymer complex as observed in Figure 10 A&B. Similar

experiment was performed with coumarin. In this case, we observed that at pH 7, the fluorescence intensity initially localized in the coacervates decreased, indicating that this dye was released in the water phase.

In a second approach, the dyes (coumarin or polystyrene beads) were introduced after the addition of calcium, and after pH was fixed at 7. For both components, there was no uptake within coacervates and the continuous phase was fluorescent. Using this pathway, the presence of the calcium seemed to act as a barrier for the penetration of these dyes, which could be due either to the charge reversal of the coacervates or to their higher cross-linking density related to ionic bridges. Obviously, encapsulation in  $\text{Ca}^{2+}$ -stabilized coacervates is pathway-dependent, meaning that  $\text{Ca}^{2+}$  distribution did not reach the same state depending on the presence or the absence of cargo.

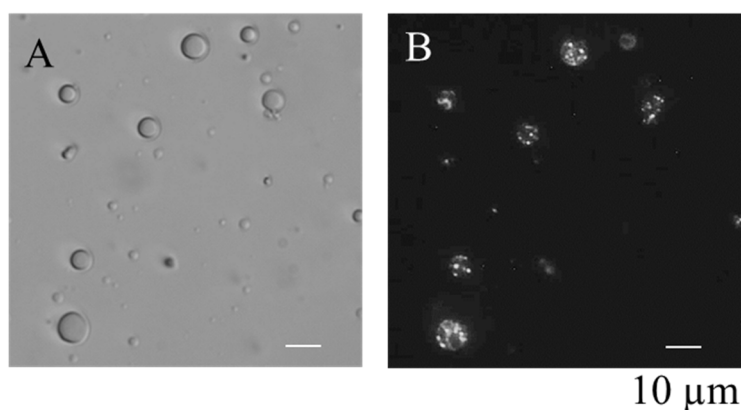


Figure 10 : A) & B) Optical and fluorescence microscopy images of coacervates in presence of fluorescently labeled polystyrene at pH = 7.

## Conclusion

This work has demonstrated that ampholyte polymer chains exhibit self-coacervation at specific positive to negative charges ratio. As in complex coacervation, this phase separation phenomenon is reversible leading to metastable droplet states or transient compartmentalized structures. Interestingly, a large variety of entities, ranging from small molecules to micrometric colloids, are spontaneously sequestered into these coacervates. The partition coefficient results from an equilibrium involving charges, dimension and hydrophobicity as in complex coacervation. [43]

A focal point of this feature lies in the generation of simple coacervates involving a unique ampholyte, which avoids mixing problem and formulation pathway. As an

illustration, C. Schatz *et al.* have pointed out the underestimated formulation pathway in complex coacervation by investigating the role of the addition of the positive chains into negative ones or the reverse. They have demonstrated that while the final morphology of coacervates should not depend on the pathway due to its equilibrium nature, it happens via a two-step process involving the formation of polyelectrolyte complex precursors. The sign and magnitude of the charge of those polyelectrolyte complexes nanoparticle precursors, which are related to the order of addition, can influence the energy cost to achieve their condensation into neutral coacervate droplets [44]. In the case of self-coacervation, the process should be of less importance due to the presence of positive and negative charges on the same chain, but their respective distribution along the chain, provided by the chemistry of the ampholyte chain, should be of prime importance. In our case, the residual surface charges were exploited to increase the robustness of the coacervates by ionic gelation of the polymer droplets. Finally, self-coacervation of polyampholytes constitutes a synthetic model for understanding phenomena occurring in nature [45] and in particular in proteins, which have the ability to form simple-coacervate.[46,47] This approach constitutes a highly promising route toward the formation of highly structured polymeric self-assembly in all-aqueous media that could be used in drug delivery, sensing or biological mimic.

### Acknowledgments

Lauriane Giraud gratification was supported by INP grant. Sharvina Shanmugathan was supported by the Chaire auto-assemblage, Fondation de Bordeaux/Solvay. The authors would like to thank E. Khetsomphou for additional experiments.

### Supplementary Material

**Figure S1:**  $^1\text{H-NMR}$  spectra of PAA before the functionalization and after the grafted of 10% of diamine. A) N,N'-dimethylethylenediamine (DA), B) Polyacrylic acid (PAA), C) PAA-DA<sub>10</sub>. **Figure S2:** Size distribution of the coacervates over 200 coacervates. PAA-DA<sub>20</sub> Mean=3.5 $\mu\text{m}$ . **Figure S3:** A) Microscopic image of the sediment after a centrifugation process at 500 rpm during 10 minutes (PAA-DA<sub>15</sub>) Large polymer rich domains are observed onto the glass slide, which are characteristic to a macroscopic phase separation. B) Direct and reverse potentiometric titration of PAA-DA<sub>15</sub> (0.25 mM). **Figure S4:** Charge surface measurements of PAA-DA<sub>15</sub> as a function of the pH. **Figure S5:** Optical microscopy image of a solution of PAA-DA<sub>15</sub> at a pH A) 4.15, B) 3.80. **Figure S6:** Size distribution of the

coacervates (PAA-DA<sub>20</sub>) after 1 and 12 days. **Figure S7:** Microscopic image of a solution of PAA-DA<sub>15</sub> stabilized by Ca<sup>2+</sup>, dispersed in deionized water after 18 days. **Table S1:** Quantification of the grafting density from the NMR spectra. **Table S2:** Microscopic pictures of coacervates loaded with various molecules. **Table S3:** Sequestration efficiency of fluorescent components determined by fluorescence spectroscopy.

## References

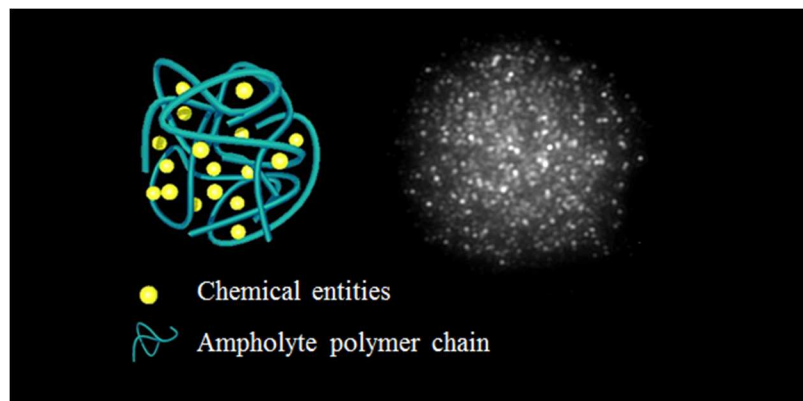
- 
- [1] C. E. Sing, *Development of the Modern Theory of Polymeric Complex Coacervation*, Adv. Colloid Interface Sci. **239** (2017) 2-16. DOI: 10.1016/j.cis.2016.04.004
- [2] W. Zhao, Y. Wang, *Coacervation with Surfactants: From Single-chain Surfactants to Gemini Surfactants*, Adv. Colloid Interface Sci. **239** (2017) 199-212. DOI: 10.1016/j.cis.2016.04.005
- [3] W. C. Blocher, S. L. Perry, *Complex Coacervate-based Materials for Biomedicine*, Nanomed. Nanobiotechnol. **9** (2017) e1442. DOI: 10.1002/wnan.1442
- [4] J.-P. Douliez, N. Martin, C. Gaillard, T. Beneyton, J.-C. Baret, S. Mann, L. Beven, *Cationic Coacervate Droplets as a Surfactant-Based Membrane-Free Protocell Model*, Angew. Chem., Int. Ed. **56** (2017) 13689-13693. DOI: 10.1002/anie.201707139
- [5] D. Garenne, L. Beven, L. Navailles, F. Nallet, E. Dufourc, J.-P. Douliez, *Sequestration of Proteins by Fatty Acid Coacervates for Their Encapsulation within Vesicles*, Angew. Chem., Int. Ed., **55**(43) (2016) 13475-13479. DOI: 10.1002/anie.201607117
- [6] Q. Wang, J. B. Schlenoff, *The Polyelectrolyte Complex/Coacervate Continuum*, Macromolecules, **47** (2014) 3108–3116. DOI: 10.1021/ma500500q
- [7] L.-W. Chang, T. K. Lytle, M. Radhakrishna, J. J. Madinya, J. Vélez, C. E. Sing, S. L. Perry, *Sequence and Entropy-based Control of Complex Coacervates*, Nat. Commun., **8** (2017) 1273. DOI: 10.1038/s41467-017-01249
- [8] M. Wang, Y. Wang, *Development of Surfactant Coacervation in Aqueous Solution*, Soft Matter, **10** (2014) 7909. DOI: 10.1039/C4SM01386G
- [9] Z. Ou, M. Muthukumar, *Entropy and Enthalpy of Polyelectrolyte Complexation: Langevin Dynamics Simulations*, J. Chem. Phys. **124** (2006) 154902. DOI: 10.1063/1.2178803
- [10] K. T. Delaney, G. H. Fredrickson, *Theory of Polyelectrolyte Complexation-Complex Coacervates are Self-coacervates*, J. Chem. Phys. **146** (2017) 224902. DOI: 10.1063/1.4985568
- [11] D. van Swaay, T.-Y. D. Tang, S. Mann, A. de Mello, *Microfluidic Formation of Membrane-Free Aqueous Coacervate Droplets in Water*, Angew. Chem. Int. Ed., **54** (2015) 8398–8401. DOI: 10.1002/anie.201502886
- [12] E. Das, K. Matsumura, *Tunable Phase-Separation Behavior of Thermoresponsive Polyampholytes Through Molecular Design*, J. Polym. Sci., Part A: Polym. Chem., **55** (2017) 876-884. DOI: 10.1002/pola.28440
- [13] Y. Xia, M. Gao, Y. Chen, X. Jia, D. Liang, *Mimic of Protein: A Highly pH-Sensitive and Thermoresponsive Polyampholyte*, Macromol. Chem. Phys., **212** (2011) 2268-2274. DOI: 10.1002/macp.201100352
- [14] H. Cai, B. Gabryelczyk, M. S. S. Manimekalai, G. Grüber, S. Salentinig, A. Miserez, *Self-Coacervation of Modular Squid Beak Proteins – a Comparative Study*, Soft Matter, **13** (2017) 7740-7752. DOI: 10.1039/c7sm01352c
- [15] S. E. Reichheld, L. D. Muiznieks, F. W. Keeley, S. Sharpe, *Direct Observation of Structure and Dynamics During Phase Separation of an Elastomeric Protein*, PNAS, **114** (2017) E4408-E4415. DOI: 10.1073/pnas.1701877114
- [16] S. Kim, H. Y. Yoo, J. Huang, Y. Lee, S. Park, Y. Park, S. Jin, Y. M. Jung, H. Zeng, D. S. Hwang, J. Yong Seok, *Salt Triggers the Simple Coacervation of an Underwater Adhesive When Cations Meet Aromatic  $\pi$  Electrons in Seawater*, ACS Nano, **11** (2017) 6764-6772. DOI: 10.1021/acsnano.7b01370
- [17] W. Wei, Y. Tan, N. R. Martinez Rodriguez, J. Yu, J. N. Israelachvili, J. H. Waite, *A Mussel-Derived One Component Adhesive Coacervate*, Acta Biomater. **10** (2014) 1663-1670. DOI: 10.1016/j.actbio.2013.09.007
- [18] I. Kaminker, W. Wei, A. M. Schrader, Y. Talmon, M. T. Valentine, J. N. Israelachvili, J. H. Waite, S. Han, *Simple Peptide Coacervates Adapted for Rapid Pressure-sensitive Wet Adhesion*, Soft Matter, **13** (2017) 9122-9131. DOI: 10.1039/c7sm01915g



- 
- [19] F. Comert, A. J. Malanowski, F. Azarikia, P. L. Dubin, *Coacervation and Precipitation in Polysaccharide-Protein Systems*, *Soft Matter*, **12** (2016) 4154-4161. DOI: 10.1039/c6sm00044d
- [20] F. Comert, D. Nguyen, M. Rushanan, P. Milas, A. Y. Xu, P. L. Dubin, *Precipitate-Coacervate Transformation in Polyelectrolyte-Mixed Micelle Systems*, *J. Phys. Chem. B*, **121** (2017) 4466-4473. DOI: 10.1021/acs.jpcc.6b12895
- [21] S.L. Turgeon, C. Schmitt, C. Sanchez, *Protein-Polysaccharide Complexes and Coacervates*, *Curr. Opin. Colloid Interface Sci.*, **12** (2007) 166-178. DOI: 10.1016/j.cocis.2007.07.007
- [22] J. R. Vieregg, T-Y D. Tang, *Polynucleotides in cellular mimics: Coacervates and lipid vesicles*, *Curr. Opin. Colloid Interface Sci.*, **26** (2016) 50-57. DOI: 10.1016/j.cocis.2016.09.004
- [23] A.J. Dzieciol, S. Mann, *Designs for Life: Protocell Models in the Laboratory*, *Chem. Soc. Rev.*, **41** (2012) 79-85. DOI: 10.1039/c1cs15211d
- [24] W. M. Aumiller, F. P. Cakmak, B. W. Davis, C. D. Keating, *RNA-Based Coacervates as a Model for Membraneless Organelles: Formation, Properties, and Interfacial Liposome Assembly*, *Langmuir*, **32** (2016) 10042-10053. DOI: 10.1021/acs.langmuir.6b02499
- [25] A. F. Mason, B. C. Buddingh, D. S. Williams, J. C. M. van Hest, *Hierarchical Self-Assembly of a Copolymer-Stabilized Coacervate Protocell*, *J. Am. Chem. Soc.*, **139** (2017) 17309-17312. DOI: 10.1021/jacs.7b10846
- [26] A. Perro, G. Meng, J. Fung, V. N. Manoharan, *Design and Synthesis of Model Transparent Aqueous Colloids with Optimal Scattering Properties*, *Langmuir*, **25** (2009) 11295-11298. DOI: 10.1021/la902861x
- [27] A. B. Kayitmazer, A. F. Koksala, E. Kilic Iyilik, *Complex Coacervation of Hyaluronic Acid and Chitosan: Effects of pH, Ionic Strength, Charge Density, Chain Length and the Charge Ratio*, *Soft Matter*, **11** (2015) 8605-8612. DOI: 10.1039/c5sm01829c
- [28] F. Comert, P. L. Dubin, *Liquid-Liquid to Liquid-Solid Phase Separation: A Transition from Rain to Snow*, *Adv. Colloid Interface Sci.*, **239** (2017) 213-217. DOI: 10.1016/j.cis.2016.08.005
- [29] X. Liu, J.-P. Chapel, C. Schatz, *Structure, Thermodynamic and Kinetic Signatures of a Synthetic Polyelectrolyte Coacervating System*, *Adv. Colloid Interface Sci.*, **239** (2017) 178-186. DOI: 10.1016/j.cis.2016.10.004
- [30] J. C. Cameselle, J. Meireles Ribeiro, A. Sillero, *Derivation and Use of a Formula to Calculate the Net Charge of Acid-Base Compounds. Its Application to Amino Acids, Proteins and Nucleotides*, *Biochem. Educ.*, **14** (1986) 131-136.
- [31] P.G. De Gennes, P. Pincus, R.M. Velasco, F. Brochard, *Remarks on Polyelectrolyte Conformation*, *J. Phys. France*, **37** (1976) 1461-1473. DOI: 10.1051/jphys:0197600370120146100
- [32] M. Castelnovo, J. F. Joanny, *Phase Diagram of Diblock Polyampholyte Solutions*, *Macromolecules*, **35** (2002) 4531-4538. DOI: 10.1021/ma012097v
- [33] C. G. de Kruif, F. Weinbreck, R. de Vries, *Complex Coacervation of Proteins and Anionic Polysaccharides*, *Curr. Opin. Colloid Interface Sci.*, **9** (2004) 340-349. DOI: 10.1016/j.cocis.2004.09.006
- [34] Y. Yin, L. Niu, X. Zhu, M. Zhao, Z. Zhang, S. Mann, D. Liang, *Non-Equilibrium Behaviour in Coacervate-Based Protocells under Electric-Field-Induced Excitation*, *Nat. Commun.*, **7**, (2016) 10658. DOI: 10.1038/ncomms10658
- [35] Y. Yin, H. Chang, H. Jing, Z. Zhang, D. Yan, S. Mann, D. Liang, *Electric Field-Induced Circulation and Vacuolization Regulate Enzyme Reactions in Coacervate-Based Protocells*, *Soft Matter*, **14** (2018) 6514-6520. DOI: 10.1039/C8SM01168K
- [36] D. S. Williams, S. Koga, C. R. C. Hak, A. Majrekar, A. J. Patil, A. W. Perriman, S. Mann, *Polymer/nucleotide Droplets as Bio-Inspired Functional Micro-Compartments*, *Soft Matter*, **8** (2012) 6004-6014. DOI: 10.1039/c2sm25184a
- [37] M. Li, X. Huang, T-Y D. Tang, S. Mann, *Synthetic Cellularity Based on Non-Lipid Micro-Compartments and Protocell Models*, *Curr. Opin. Chem. Biol.* **22** (2014) 1-11. DOI: 10.1016/j.cbpa.2014.05.018
- [38] C. D. Keating, *Aqueous Phase Separation as a Possible Route to Compartmentalization of Biological Molecules*, *Accounts in Chemical Research*, **45** (2012) 2114-2124. DOI: 10.1021/ar200294y

- 
- [39] D. N. Cacace, A. T. Rowland, J. J. Stapleton, D. C. Dewey, C. D. Keating, *Aqueous Emulsion Droplets Stabilized by Lipid Vesicles as Microcompartments for Biomimetic Mineralization*, *Langmuir*, **31** (2015) 11329-11338. DOI: 10.1021/acs.langmuir.5b02754
- [40] V. Vao-soongnern, K. Merat, S. Horpibulsuk, *Interaction of the Calcium Ion with Poly(acrylic acid) as Investigated by a Combination of Molecular Dynamics Simulation and X-ray Absorption Spectroscopy*, *J. Polym. Res.* **23** (2016) 7. DOI: 10.1007/s10965-015-0895-z
- [41] J. P. Douliez, A. Perro, J. P. Chapel, B. Goudeau, L. Béven, *Preparation of Template-Free Robust Yolk-Shell Gelled Particles from Controllably Evolved All-in-Water Emulsions*, *Small*, **14** (2018) e1803042. DOI: 10.1002/smll.201803042
- [42] K. K. Nakashima, J. F. Baaij, E. Spruijt, *Reversible Generation of Coacervate Droplets in an Enzymatic Network*, *Soft Matter*, **14** (2018) 361-367. DOI: 10.1039/c7sm01897e
- [43] M. Zhao, N. S. Zacharia, *Sequestration of Methylene Blue into Polyelectrolyte Complex Coacervates*, *Macromol. Rapid Commun.*, **37** (2016) 1249-1255. DOI: 10.1002/marc.201600244
- [44] X. Liu, J.-P. Chapel, C. Schatz, *Structure, thermodynamic and kinetic signatures of a synthetic polyelectrolyte coacervating system*, *Adv. Colloid Interface Sci.*, **239** (2017) 178–186. DOI: 10.1016/j.cis.2016.10.004
- [45] A. I. Oparin, *The origin of life*, New York, 1953.
- [46] P. Mohammadi, G. Beaune, B. T. Stokke, J. V. I. Timonen, M. B. Linder, *Self-Coacervation of a Silk-Like Protein and Its Use As an Adhesive for Cellulosic Materials*, *ACS Macro Lett.* **7** (2018) 1120–1125. DOI: 10.1021/acsmacrolett.8b00527
- [47] P. K. Forooshani, B. P Lee, *Recent approaches in designing bioadhesive materials inspired by mussel adhesive protein*, *J. Polym. Sci., Part A: Polym. Chem.* **55** (2016) 9-33. DOI: 10.1002/pola.28368

## Graphical Abstract



## Supplementary Material

### Self-coacervation of ampholyte polymer chains as an efficient encapsulation strategy

Adeline Perro<sup>1,\*</sup>, Lauriane Giraud<sup>1</sup>, Noémie Coudon<sup>1</sup>, Sharvina Shanmugathasan<sup>1</sup>, Véronique Lapeyre<sup>1</sup>, Bertrand Goudeau<sup>1</sup> Jean-Paul Douliez<sup>2</sup> and Valérie Ravaine<sup>1</sup>

<sup>1</sup> Université de Bordeaux, Bordeaux INP, ISM, UMR 5255, Site ENSCBP, 16 avenue Pey Berland, 33607 Pessac, France.

<sup>2</sup> UMR1332, Biologie du Fruit et Pathologie, INRA, univ. Bordeaux, Centre de Bordeaux, 33883, Villenave d'Ornon, France.

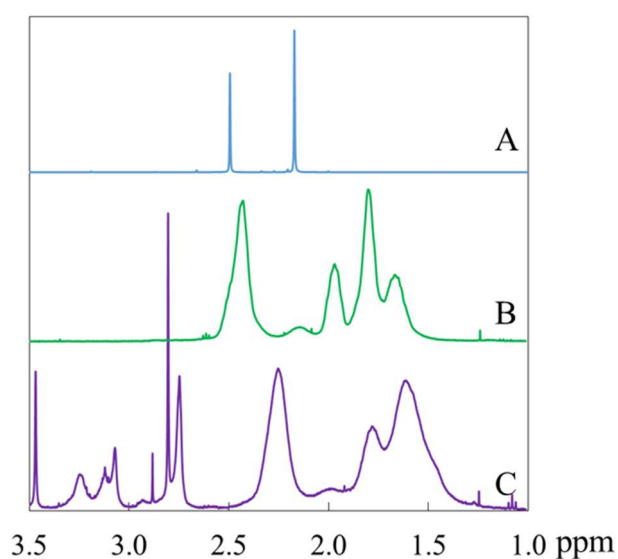
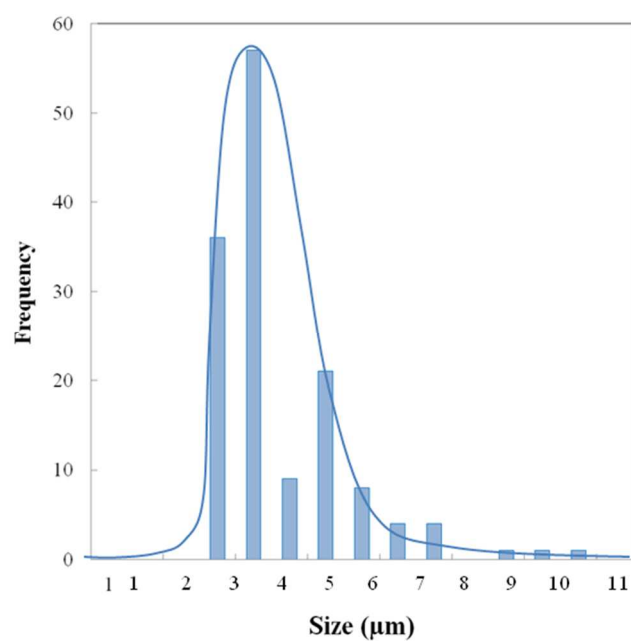


**Figure S1:** <sup>1</sup>H-NMR spectra of PAA before the functionalization and after the grafted of 10% of diamine. A) N,N'-dimethylethylenediamine (DA), B) Polyacrylic acid (PAA), C) PAA-DA<sub>10</sub>.

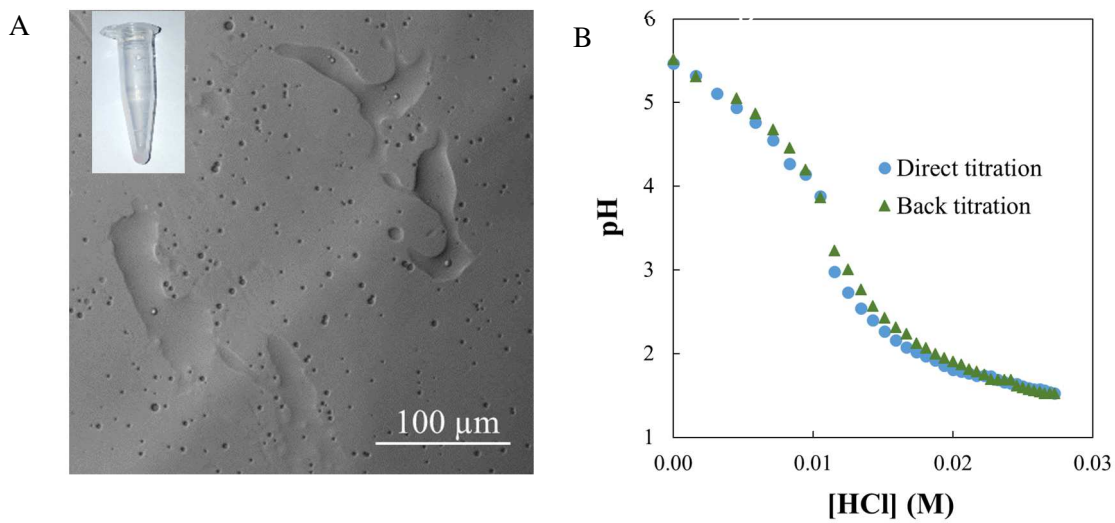
**Table S1:** Quantification of the grafting density from the NMR spectra.

	a (1.3-2 ppm)	b (2-2.5 ppm)	c + d (3-3.4 ppm)	Grafting density (%)
Number of protons	4	2	4	
PAA	0.65	0.35		
PAA-DA <sub>5</sub>	0.63	0.33	0.04	3.6
PAA-DA <sub>10</sub>	0.58	0.30	0.12	10.1
PAA-DA <sub>15</sub>	0.58	0.25	0.17	16.5
PAA-DA <sub>20</sub>	0.55	0.25	0.20	18.5
PAA-DA <sub>25</sub>	0.54	0.25	0.20	27.4
PAA-DA <sub>30</sub>	0.53	0.13	0.34	31.6
PAA-DA <sub>40</sub>	0.49	0.11	0.40	66.0

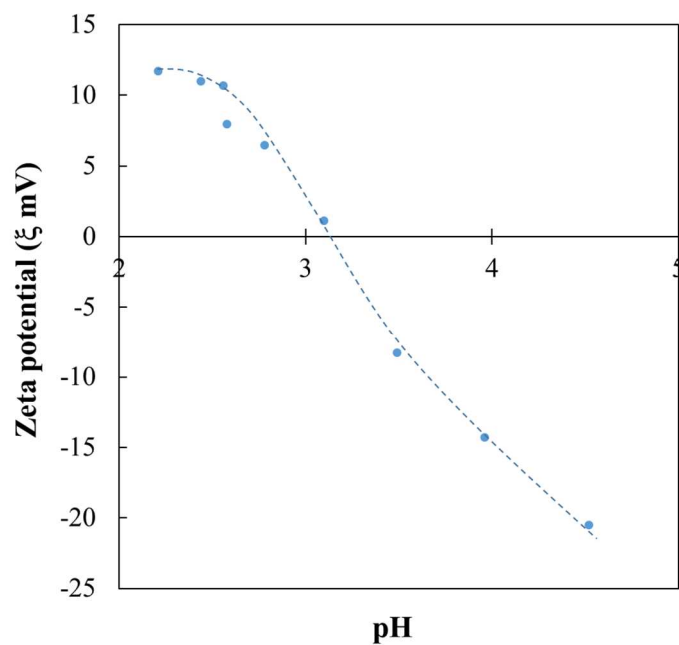
The sum of integration peaks was normalized to 1. The calculations were performed considering the mean of the ratios  $a/(c+d)$  and  $b/(c+d)$ .



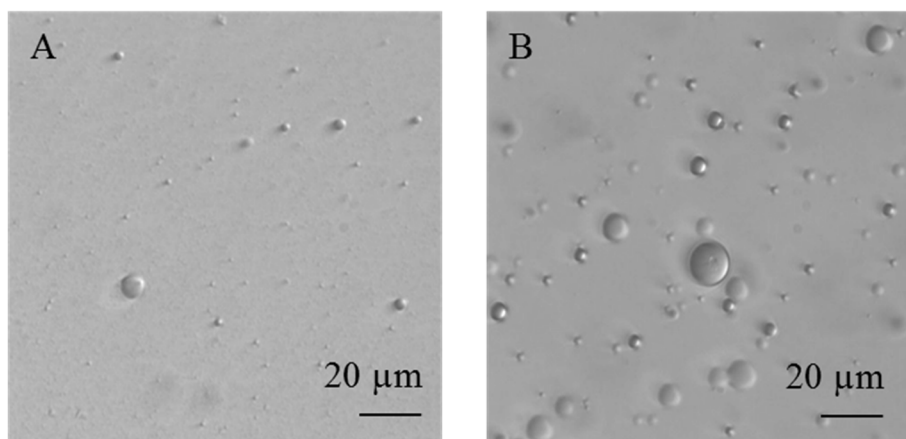
**Figure S2:** Size distribution of the coacervates over 200 coacervates. PAA-DA<sub>20</sub> Mean=3.5µm.



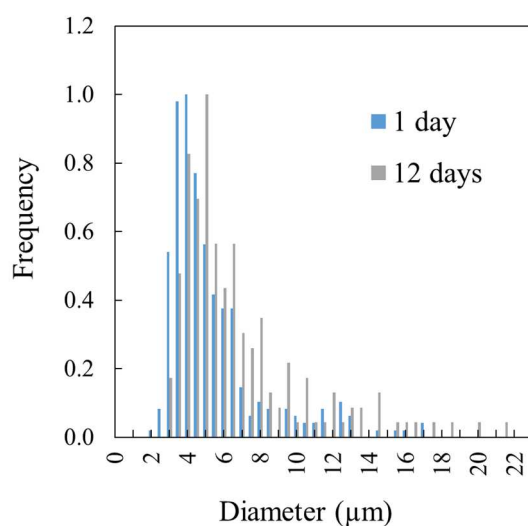
**Figure S3:** A) Microscopic image of the sediment after a centrifugation process at 500 rpm during 10 minutes (PAA-DA<sub>15</sub>). Large polymer rich domains are observed onto the glass slide, which are characteristic to a macroscopic phase separation. B) Direct and reverse potentiometric titration of PAA-DA<sub>15</sub> (0.25 mM).



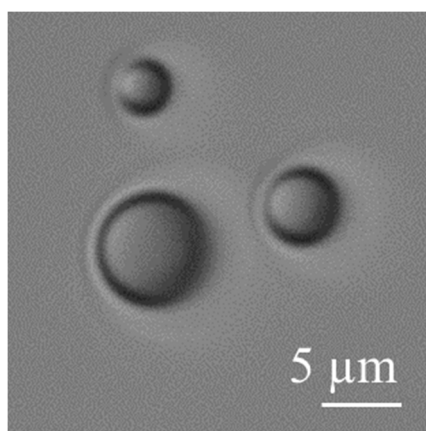
**Figure S4:** Charge surface measurements of PAA-DA<sub>15</sub> as a function of the pH.



**Figure S5:** Optical microscopy image of a solution of PAA-DA<sub>15</sub> at a pH A) 4.15, B) 3.80.

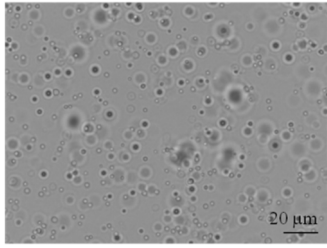
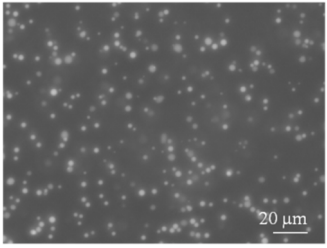
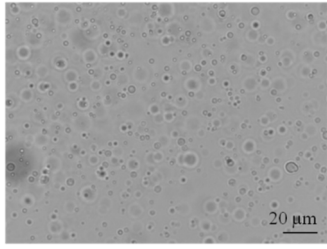
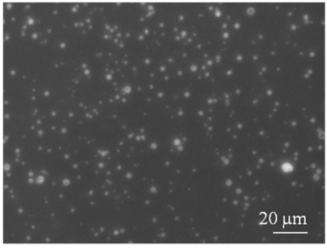
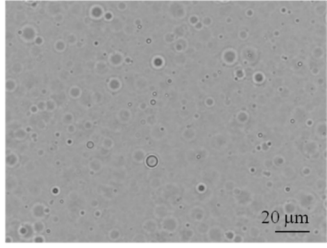
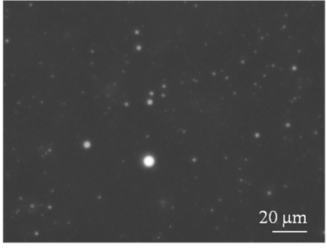
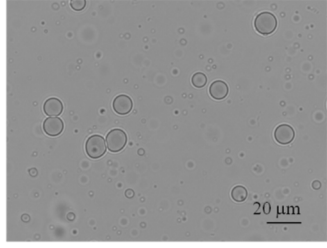
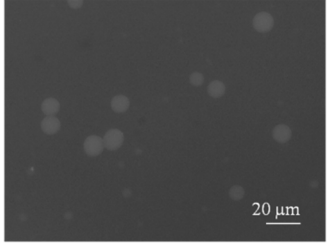
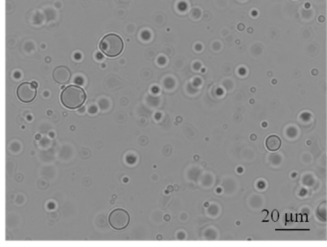
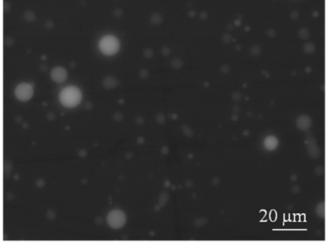
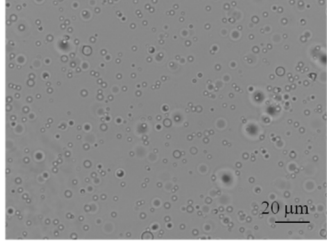
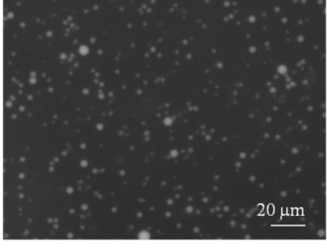


**Figure S6:** Size distribution of the coacervates (PAA-DA<sub>20</sub>) after 1 and 12 days.



**Figure S7:** Microscopic image of a solution of PAA-DA<sub>15</sub> stabilized by Ca<sup>2+</sup>, dispersed in deionized water after 18 days.

Table S2: Microscopic pictures of coacervates loaded with various molecules.

Name	Mol wt.	Charge	Bright Field	Fluorescence
Rhodamine B	479	+		
FITC	389	-		
DEAE Dextran-FITC	150k	+		
CM Dextran-FITC	150k	-		
Dextran-Rhodamine B	10k	0		
Dextran-Rhodamine B	70k	0		

\* Droplets of coacervates were observed without any purification process.



Table S3: Sequestration efficiency of fluorescent components determined by fluorescence spectroscopy.

Name	Mol wt.	$I_{\text{Fluo}}$ in absence of coacervates	$I_{\text{Fluo}}$ in presence of coacervates	Sequestration efficiency
Rhodamine B	479	404	150	63
Dextran Rho. B	10 000	90	64	29
Dextran Rho. B	70 000	108	87	19